Acta Cryst. (1970). A**26**, 367

A New Method for Evaluating Slit-Smeared Small Angle X-ray Scattering Data

BY G. R. STROBL

Institut für Physikalische Chemie der Universität Mainz, Germany

(*Received* 12 *June* 1969)

A new method for evaluating slit-smeared small-angle scattering data is discussed. It is applicable to any primary beam-intensity distribution. The propagation of measuring errors is examined; expressions for the computation of the precision of all derived pinhole scattering curve properties are given. There is no need to smooth the measured curve before applying the evaluation procedures. The method turns out to be very suitable for practical use.

Introduction

To examine X-ray scattering in the small-angle range slit-collimation systems are normally used. For the registration of the scattered intensity in a plane perpendicular to the primary beam plane counting detectors with a slit-like window are often used. The experimental result, the 'slit-smeared' scattering curve, does not show the interesting diffraction intensity distribution in reciprocal space. A measurement made with the counter window at height h above the primary beam plane records an integral intensity $\tilde{S}(h)$, which in the case of an isotropic sample can be expressed as

$$\tilde{S}(h) = \int_{b=h}^{\infty} g(h, b) S_0(b) \mathrm{d}b \,. \tag{1}$$

Here $S_0(b)$ is the corresponding pinhole scattering intensity distribution in the plane of registration and $g(h, b)$ is a weighting function which depends upon the collimation- and registration-system geometries.

Methods for calculating $S_0(b)$ from the measured slit-smeared scattering curve, *i.e.*, solving the smearing equation (1) for the unknown function $S_0(b)$, have been published by various authors. Guinier & Fournet (1947) and DuMond (1947) found an analytical solution for the case of a primary beam of infinite slit-height. Modifications of this method for use with various slit collimation geometries have been developed by Kratky, Porod & Kahovec (1951), Gerold (1957), Schmidt & Hight (1960), Heine & Roppert (1962), Kent & Brumberger (1964) and others. A Fourier transform method has been described by Ruland (1964).

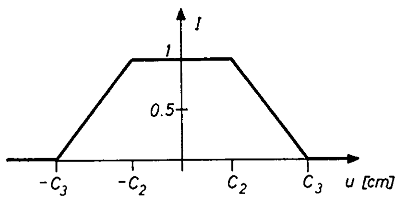

Fig. 1. Primary beam intensity distribution.

Recently some new approaches to the problem have been published: Mazur & Wims (1966) established a formal method for solving the smearing integral equation, Lake (1967) has treated it by an iteration procedure, and Hossfeld (1968) has developed an algebra in coefficients of Hermite polynomials.

In the following sections a new method for evaluating slit-smeared scattering data is discussed. The method is applicable to arbitrary primary beam intensity distributions and allows the calculation of averages over the pinhole scattering values within distinct regions (with the limiting case of local values of the pinhole scattering curve), and the computation of the electron density autocorrelation function.

It can be shown that small changes in the values of the smeared curve are generally related to considerable changes in the pinhole scattering curve. As a consequence errors in the smeared curve may result in quite large deviations of the calculated pinhole scattering curve from its true form. To obtain knowledge of the precision of the calculated quantities the propagation of errors has been examined. Expressions for the computation of the precision of all calculated quantities are given. The most important advantage of the method discussed is that, using these expressions, the information content of the measurement can be judged.

In addition, in contrast to most of the existing methods, the present method employs the measured data directly without any preceding smoothing procedures. It is therefore very suitable for practical application.

The smearing equation

Generally the weighting function $g(h, b)$ is determined by the primary-beam intensity distribution in the registration plane and the dimensions of the counter window. In our case, where the widths of the primary beam and the counter window are negligibly small compared with their heights, the critical parameters are the height of the counter window, $2C_1$, and the primary beam intensity distribution along the slit, $I(u)$, which gives the intensity per unit height, expressed in relative units ($I(0) = 1$). It is easily shown that, using these parameters, the slit-smeared scattering curve $S(h)$ and the pinhole curve in the plane of registration $S_0(b)$ can be related by the equation

$$\tilde{S}(h) = \int_{u'=-\infty}^{\infty} V(u') \, . \, S_0(\sqrt{h^2+u'^2})\mathrm{d}u' \,, \qquad (2)$$

where

$$V(u') = \int_{u=u'-C_1}^{u'+C_1} I(u)\mathrm{d}u \,. \qquad (3)$$

Use of the relation $b^2 = h^2 + u'^2$ between the coordinates in the registration plane leads to the more suitable form

$$\tilde{S}(h) = \int_{b=h}^{\infty} G(b^2-h^2)S_0(b)\mathrm{d}b^2 \,, \qquad (4)$$

where

$$G(b^2-h^2) = \frac{V(\sqrt{b^2-h^2}) + V(-\sqrt{b^2-h^2})}{2\sqrt{b^2-h^2}} \,. \qquad (5)$$

Under normal experimental conditions $I(u)$ is trapezoidal and can be described, as indicated in Fig. 1, by the parameters C_2 and C_3. C_1 is normally chosen so that $C_1 < C_2$. In this, the usual case, we obtain

$$V(u) = 2C_1 \,, \quad \text{if} \quad u \le C_2 - C_1 \,.$$

As a consequence the weighting function becomes

$$G(b^2-h^2) = \frac{2C_1}{\sqrt{b^2-h^2}} \,, \text{ if } b^2-h^2 \le (C_2-C_1)^2 \qquad (6)$$

and is equal in this region to the weighting function of a homogeneous primary beam of infinite height. This

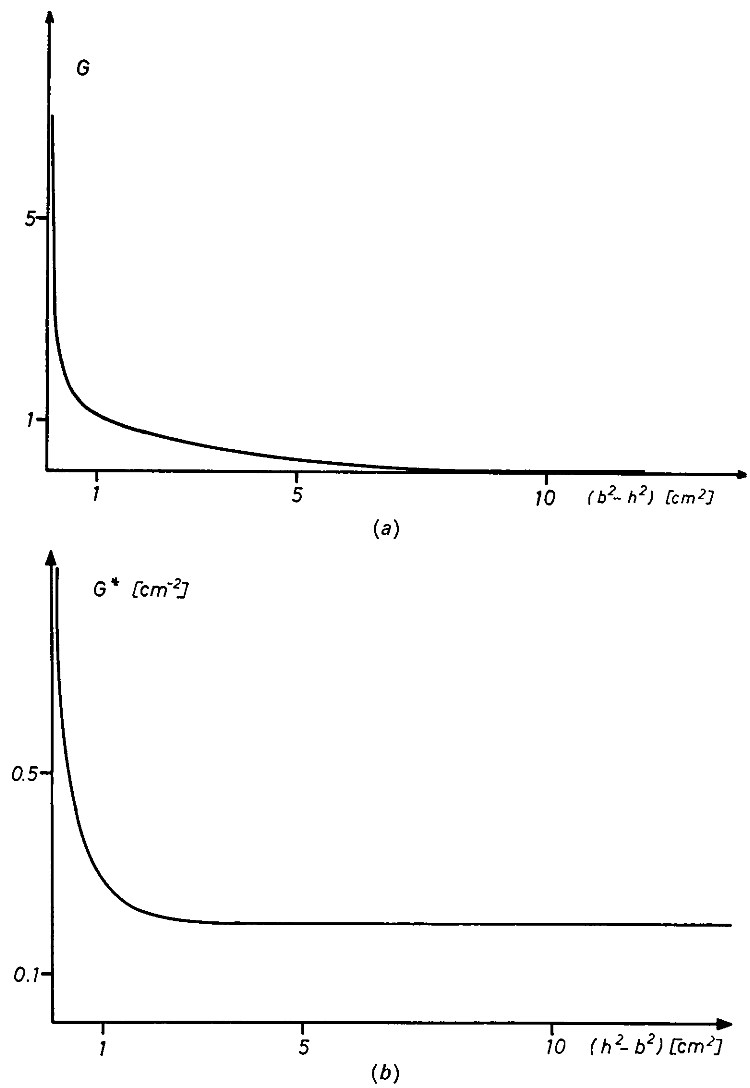

Fig. 2. (*a*) Smearing function $G(b^2-h^2)$, as calculated for parameter values $C_1 = 0{\cdot}5$, $C_2 = 1{\cdot}5$, $C_3 = 2{\cdot}9$ cm. Function (*b*) $G^*(h^2-b^2)$ corresponding to the smearing function $G(b^2-h^2)$ in (*a*).

property expresses the well known fact that the assumption of a slit of infinite height is justified only if the scattered radiation is mainly limited to the region $h^2 \leq (C_2 - C_1)^2$.

The smearing equation (4) may be transformed to an equivalent system of linear equations

$$\tilde{\mathbf{S}} = \bar{\mathbf{g}} \, . \, d \, . \, \bar{\mathbf{S}}_0 \tag{7}$$

with

$$\tilde{\mathbf{S}} = [\tilde{S}(h_i)] \, ; \quad \bar{\mathbf{S}}_0 = [\bar{S}_0(b_i)]$$

$$\bar{\mathbf{g}} = [\bar{g}(h_i, b_j) = \frac{1}{d} \int_{b'=bj}^{bj+1} G(b'^2 - h_i^2) \mathrm{d}b'^2] \tag{8}$$

where $[b_1 = h_1 = 0,\ b_2 = h_2 = d,\ \ldots,\ b_N = h_N = (N-1)d]$ is a series of N equidistant points and $\bar{S}_0(b_i)$ is an average value with limits

$$S_0(b_i) \leq \bar{S}_0(b_i) \leq S_0(b_{i+1}) \, .$$

In principle, the system of linear equations (7) can be solved for the unknown quantity $\bar{\mathbf{S}}_0$. However, since there is some uncertainty in the determination of $\tilde{\mathbf{S}}$ due to measuring errors of random character, the corresponding uncertainty in $\bar{\mathbf{S}}_0$ should be examined. An upper limit for this uncertainty in $\bar{\mathbf{S}}_0$ is given, using the condition-number $\mathrm{cond}_\infty(\bar{\mathbf{g}})$ (see, *e.g.* Franklin, 1968)

$$\frac{|\delta\bar{\mathbf{S}}_0|_\infty}{|\bar{\mathbf{S}}_0|_\infty} \leq \mathrm{cond}_\infty(\bar{\mathbf{g}}) \frac{|\delta\tilde{\mathbf{S}}|_\infty}{|\tilde{\mathbf{S}}|_\infty} \, ,$$

where $\delta\bar{\mathbf{S}}_0$ is the change in $\bar{\mathbf{S}}_0$ connected with a small deviation $\delta\tilde{\mathbf{S}}$ [generally $|\mathbf{U}|_\infty$ means the Tschebyscheff-norm $\max_i |U_i|$ of a vector $\mathbf{U} = (U_i)$]. It can be shown (see Appendix) that, under normal experimental conditions and if d is sufficiently small, the condition-number is determined as

$$\mathrm{cond}_\infty(\bar{\mathbf{g}}) = \frac{C_1 \, . \, L}{d \, . \, V(0)}$$

where $L = \int_{u=-\infty}^{\infty} I(u)\mathrm{d}u$ is a measure of the height of the primary beam.

As a consequence it is found that, if d takes small values, a slight uncertainty in $\tilde{\mathbf{S}}$ is greatly magnified and can result in a considerable uncertainty in $\bar{\mathbf{S}}_0$. There is another interesting result: suppose we want to determine $\bar{\mathbf{S}}_0$ with a certain precision. We may say that, for the measurement time t_M, needed to arrive at this precision, the following proportionality relation is valid:

$$t_M \sim \frac{\mathrm{cond}_\infty(\bar{\mathbf{g}})}{\text{total intensity of the primary beam} \times \text{height of the counter window}}$$

$$\simeq \frac{C_1 \, . \, L}{d \, . \, V(0) \, . \, L \, . \, C_1} = \frac{1}{d \, . \int_{u=-C_1}^{C_1} I(u)\mathrm{d}u} \, . \tag{9}$$

Equation (9) means that in order to shorten the measuring time, the smaller of the two parameters C_1, C_3 must be increased.

Method of solution

It is possible to compute from the smeared scattering curve $\tilde{S}(h)$, by a simple convolution procedure, values of the integral intensity $T(b)$, defined by

$$T(b) = \int_{b'=b}^{\infty} S_0(b')\mathrm{d}b'^2 \, . \tag{10}$$

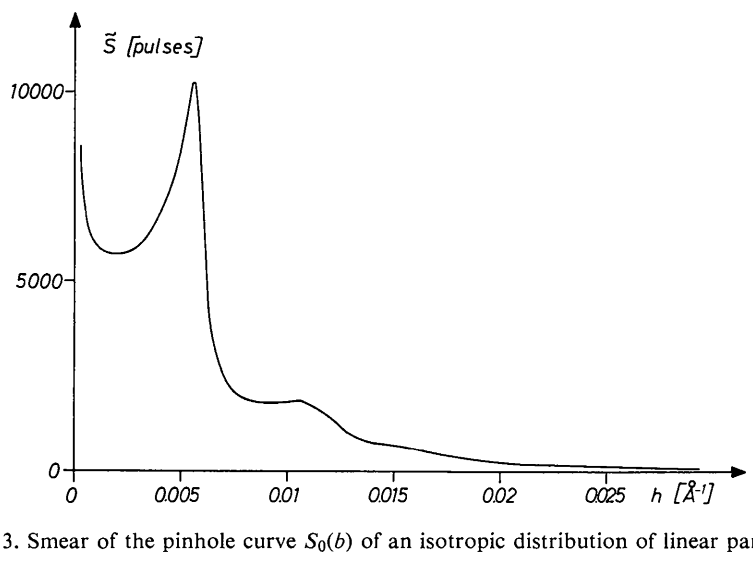

Fig. 3. Smear of the pinhole curve $S_0(b)$ of an isotropic distribution of linear paracrystals.

This can be demonstrated as follows.

Multiplication of equation (4) by a function $G^*(h^2-b'^2)$ and integration lead to

$$\int_{h=b'}^{\infty} G^*(h^2-b'^2)\tilde{S}(h)\mathrm{d}h^2 = \int_{h=b'}^{\infty}\int_{b=h}^{\infty} G^*(h^2-b'^2)G(b^2-h^2)S_0(b)\mathrm{d}h^2\mathrm{d}b^2 .$$

Rearranging the integration order we obtain

$$\int_{h=b'}^{\infty} G^*(h^2-b'^2)\tilde{S}(h)\mathrm{d}h^2 = \int_{b=b'}^{\infty} S_0(b)\left(\int_{h=b'}^{b} G^*(h^2-b'^2)G(b^2-h^2)\mathrm{d}h^2\right)\mathrm{d}b^2 .$$

If G^* is now determined by the condition

$$\int_{h=b'}^{b} G^*(h^2-b'^2)G(b^2-h^2)\mathrm{d}h^2 = \mathrm{const}\,(b'^2, b^2) = 1$$

or

$$\int_{t'=0}^{t} G^*(t')G(t-t')\mathrm{d}t' = \mathrm{const}\,(t) = 1 \qquad (11)$$

we arrive at the relation

$$T(b) = \int_{h=b}^{\infty} G^*(h^2-b^2)\tilde{S}(h)\mathrm{d}h^2 . \qquad (12)$$

Equation (12) means that the integral intensity $T(b)$ can be derived from the smeared scattering curve by convolution of $\tilde{S}(h^2)$ with the function G^*.

This function G^* can be determined as follows. For a series of equidistant points $[x_i=(i-1)d]$ equation (11) may be transformed to

$$d\sum_{i=1}^{j} \bar{G}_i^*\bar{G}_{j-i+1} = 1 , \quad j=1,2,\ldots,j_m \qquad (13)$$

where $\bar{G}_i^*$, $\bar{G}_i$ are average values with properties

$$G[(i-1)\,.\,d] \le \bar{G}_i \le G(i\,.\,d) ;$$

$$G^*[(i-1)\,.\,d] \le \bar{G}_i^* \le G^*(i\,.\,d) .$$

Equation (13) allows a successive determination of $\bar{G}_1^*$, $\bar{G}_2^*$, *etc.* By using sufficiently small values of d, $G^*(t)$ can be approximated as closely as desired.

For values of $t \le (C_1-C_2)^2$ the function $G^*(t)$ can be described by an analytical expression. We have, recalling equation (6)

$$G(t) = \frac{2C_1}{\sqrt{t}}, \quad \text{if} \quad t \le (C_1-C_2)^2 .$$

Inserting this expression in the integral equation (11) we get

$$\int_{t=0}^{t} G^*(t')\frac{2C_1}{\sqrt{t-t'}}\mathrm{d}t' = 1 , \qquad (14)$$

an equation which defines $G^*(t)$ for values of $t \le (C_1-C_2)^2$. As is well known, the solution of (14) is

$$G^*(t) = \frac{1}{2\pi C_1\sqrt{t}} . \qquad (15)$$

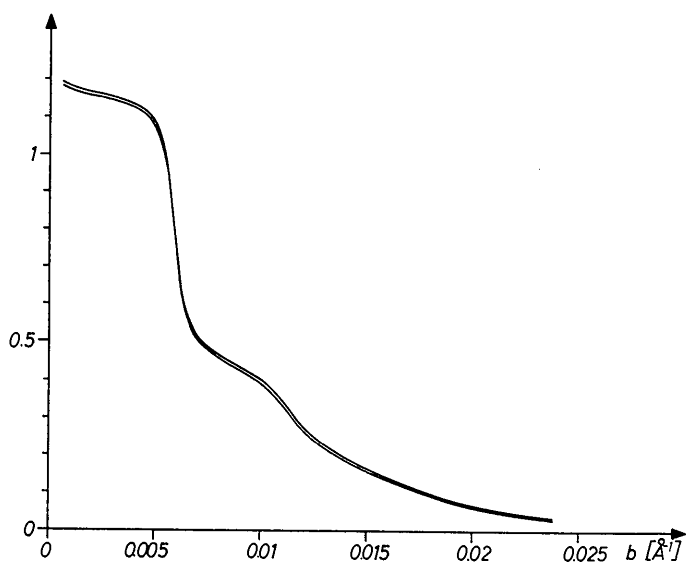

Fig. 4. Limiting curves for the integral intensity $T(b) = \int_{b'=b}^{\infty} S_0(b')\mathrm{d}b'^2$.

For sufficiently large values of t, let us say $t \geq C_4^2$, G^* can be approximated by its asymptotic value

$$G^*(t \rightarrow \infty) = 1 / \int_{t'=0}^{\infty} G(t')dt' .$$

The constant C_4 defines a 'range of influence': in order to compute

$$\int_{b_1}^{b_2} S_0(b)db^2 = T(b_1) - T(b_2)$$

or a similar integral or averaged quantities, the only requirement is information about the behaviour of $\tilde{S}(h)$ within the region $b_1^2 \leq h^2 \leq b_2^2 + C_4^2$.

As an example Fig. 2(b) shows the function G^* which has to be applied in the case of the smearing function G shown in Fig. 2(a).

It must be remarked at this point that Kratky, Porod & Kahovec (1951) have derived an integral equation which is quite closely related to our equation (11), and connects the quantities $G(t) \,.\, \sqrt{t}$, $G^*(t) \,.\, \sqrt{t}$ (called $g(t)$, $f(t)$ in their publication). This integral equation has a rather complicated form and a method of solving it for the general case could not be found.

Equation (15) shows that $G^*(t)$ tends to infinity as $t \rightarrow 0$. This singularity may be eliminated by transforming equation (12) to

$$T(b) = \int_{h=b}^{\infty} \tilde{S}(h)dF^*(h^2 - b^2) \tag{16}$$

where

$$F^*(t) = \int_{t'=0}^{t} G^*(t')dt' . \tag{17}$$

For numerical computations equation (16) is the more suitable form. For a series of N points ($h_i = b_i$) the integral (16) is evaluated by calculating sums of the type

$$T(b_i) = \sum_{j=i}^{N} g_{ij}\tilde{S}(h_j) . \tag{18}$$

Statistical analysis of error propagation

Let us now discuss the effects of errors. In view of their random nature we will treat them statistically.

Each series of N intensity measurements, expressed as pulses per minute, is represented as a point in the sample space of an N-dimensional random variable

$$\tilde{\boldsymbol{\sigma}} = [\tilde{\sigma}(h_1), \tilde{\sigma}(h_2), \ldots, \tilde{\sigma}(h_N)]$$

with the mean

$$\langle \tilde{\boldsymbol{\sigma}} \rangle = [\tilde{S}(h_1), \tilde{S}(h_2), \ldots, \tilde{S}(h_N)]$$

(the exact value of a physical quantity and the corresponding random variable, representing the possible experimental results, are distinguished by using roman or Greek letters respectively). The errors in different measured values are statistically independent. Therefore, using the abbreviation $\Delta\varepsilon = \varepsilon - \langle\varepsilon\rangle$ we have

$$\langle \Delta(\tilde{\sigma} h_i), \Delta \tilde{\sigma}(h_j) \rangle = \delta_{ij} \langle \Delta \tilde{\sigma}(h_i)^2 \rangle . \tag{19}$$

The possible experimental results form a Poisson distribution. This leads, depending upon the method of measurement, to the following expressions for the variance $\langle \Delta \tilde{\sigma}(h_i)^2 \rangle$ of $\tilde{\sigma}(h_i)$:

$$\langle \Delta \tilde{\sigma}(h_i)^2 \rangle = \frac{\langle \tilde{\sigma}(h_i) \rangle}{Q} \simeq \frac{\tilde{\sigma}(h_i)}{Q} ,$$

if the pulses during Q minutes are counted or

$$\langle \Delta \tilde{\sigma}(h_i)^2 \rangle = \frac{\langle \tilde{\sigma}(h_i) \rangle^2}{P} \simeq \frac{\tilde{\sigma}(h_i)^2}{P} ,$$

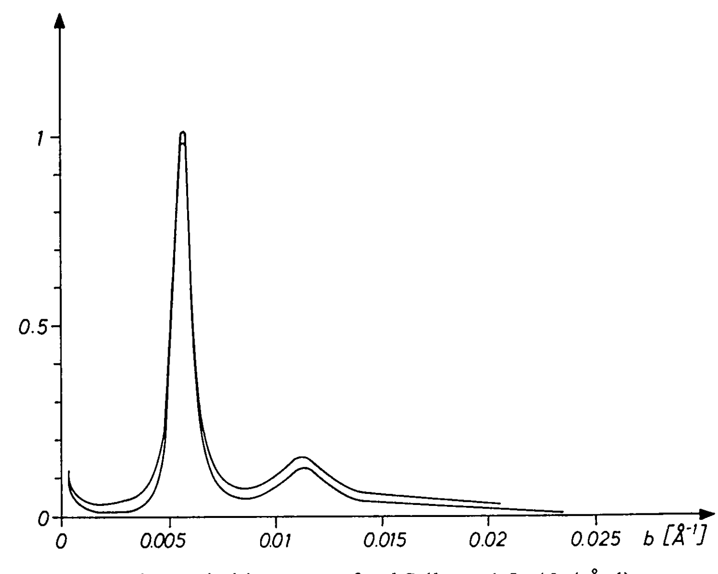

Fig. 5. Limiting curves for $bS_0(b, w = 1{,}5 \,.\, 10^{-4}\,Å^{-1})$.

if the time needed to register P pulses is measured.

In addition to $\tilde{\boldsymbol{\sigma}}$, $\boldsymbol{\tau}=[\tau(b_1), \ldots, \tau(b_N)]$, defined by

$$\tau(b_i)=\sum_{j=i}^{N} g_{ij}\tilde{\sigma}(h_j) \qquad (20)$$

is a random variable. It has the mean

$$\langle\boldsymbol{\tau}\rangle=[T(b_1), T(b_2), \ldots, T(b_N)] \qquad (21)$$

and the variance

$$\langle\Delta\tau(b_i)^2\rangle=\sum_{j=i}^{N} g_{ij}^2\langle\Delta\,\tilde{\sigma}(h_j)^2\rangle\,. \qquad (22)$$

$\tau(b_i)$, as a sum over a large number of independent variables, is approximately of Gaussian distribution. As a consequence, the major portion (86%) of sample points lies within the range

$$\langle\tau(b_i)\rangle-1{\cdot}5\sqrt{\langle\Delta\tau(b_i)^2\rangle}\rightarrow\langle\tau(b_i)\rangle+1{\cdot}5\sqrt{\langle\Delta\tau(b_i)^2\rangle}\,.$$

Using the two series of calculated quantities $[\tau(b_i)]$, $[\langle\Delta\tau(b_i)^2\rangle]$ we are now able to specify limits for $T(b)$. In the main $T(b)$ lies between the two sets of points

$$[\tau(b_i)-1{\cdot}5\sqrt{\langle\Delta\tau(b_i)^2\rangle}] \quad\text{and}\quad [\tau(b_i)+1{\cdot}5\sqrt{\langle\Delta\tau(b_i)^2\rangle}\,. \qquad (23)$$

Calculation of the autocorrelation function

Sometimes one is interested in the electron-density autocorrelation function for isotropic scatterers

$$K(r=|x|)=\frac{1}{V}\cdot\int_V \eta(x+y)\eta(y)\mathrm{d}^3y-\left(\frac{1}{V}\int_V \eta(y)\mathrm{d}^3y\right)^2,$$

where η is the electron density and V is the scattering volume.

There is a well known relation (see, *e.g.* Guinier, 1963) between $K(r)$ and the scattering intensity distribution in reciprocal space $S_0(s)$:

$$rK(r)\sim\int_{s=0}^{\infty} S_0(s)2s\,.\,\sin 2\pi sr\,.\,\mathrm{d}s\,. \qquad (24)$$

In the small angle region the reciprocal space coordinate s and the measuring system coordinate b are related by

$$s\sim b\,. \qquad (25)$$

By use of equation (25), and since from equation (10)

$$\mathrm{d}T=-2bS_0(b)\mathrm{d}b\,,$$

equation (24) may be written as

$$rK(r)=-C\int_{b=0}^{\infty}\sin 2\pi C'br\,.\,\mathrm{d}T$$

where C and C' are appropriate constants.

By partial integration, using the two properties

$$\lim_{b\to 0} T(b)\sin 2\pi C'br=0\,,\quad \lim_{b\to\infty} T(b)\sin 2\pi C'br=0\,,$$

which are valid for all real cases, we arrive at

$$K(r)=2\pi C\int_0^{\infty} T(b)\cos 2\pi C'br\,.\,\mathrm{d}b\,. \qquad (26)$$

Hence Fourier transformation of the integral intensity $T(b)$ leads to the autocorrelation function $K(r)$.

The calculation of the variance of the stochastic process $\kappa(r)$ corresponding to $K(r)$, can easely be made by a computer by evaluating the double integral

$$\langle\Delta\kappa(r)^2\rangle=(2\pi C)^2\int_b\int_{b'}\langle\Delta\tau(b)\Delta\tau(b')\rangle \times\cos 2\pi C'br\,.\,\cos 2\pi C'b'r\,.\,\mathrm{d}b\,.\,\mathrm{d}b'$$

where

$$\langle\Delta\tau(b_i)\Delta\tau(b_{j\geq i})\rangle=\sum_{j'=j}^{N} g_{ij'}g_{jj'}\langle\Delta\,\tilde{\sigma}\,(h_{j'})^2\rangle\,.$$

Evaluation methods

The first step in the evaluation of scattering data is the computation of the limits (23) for the course of the integral intensity $T(b)$ by use of the equations (20) and (22). Many interesting properties of the pinhole scattering curve, for example the position, integral intensity and peak intensity of a reflexion, can be taken directly from $T(b)$.

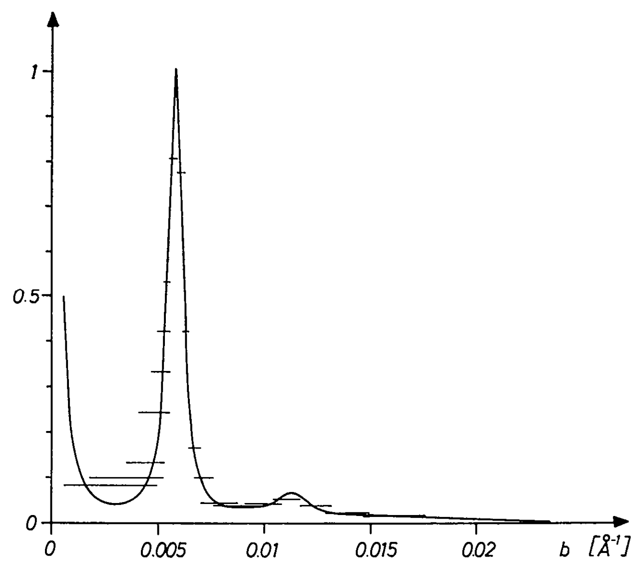

Fig. 6. Original pinhole curve. The dashes represent average values $\int_{b_1}^{b_2} S_0(b')\mathrm{d}b'^2/(b_2^2-b_1^2)$ as calculated from the smeared curve; b_1 and b_2 are indicated by the beginning and end of a dash respectively.

If necessary in a further step we can calculate averages over the pinhole scattering values within distinct regions. Let us introduce for this purpose a general notation for average values

$$\bar{U}(t, w) = \frac{1}{w}\int_{t'=t-\frac{w}{2}}^{t+\frac{w}{2}} U(t')\mathrm{d}t\,,$$

and the abbreviation

$$S_1(b) = 2b\,.\,S_0(b)\,.$$

Average values $\bar{S}_1(b, w)$ are easily derived from the integral intensity $T(b)$: using equations (10) and (18), we obtain

$$\bar{S}_1\left(\frac{b_i+b_j}{2}, b_j-b_i\right) = \frac{1}{b_j-b_i}[T(b_i)-T(b_j)]$$
$$\simeq \frac{1}{b_j-b_i}\left[\sum_{j'=i}^{j-1} g_{ij'}\tilde{\sigma}(h_{j'}) + \sum_{j'=j}^{N}(g_{ij'}-g_{jj'})\tilde{S}(h_{j'})\,.\right]$$

The corresponding random variable $\bar{\sigma}_1(b, w)$, defined by

$$\bar{\sigma}_1\left(\frac{b_i+b_j}{2}, b_j-b_i\right) = \frac{1}{b_i-b_j}[\tau(b_i)-\tau(b_j)] \quad (27)$$

has mean

$$<\bar{\sigma}_1\left(\frac{b_i+b_j}{2}, b_j-b_i\right)> = \bar{S}_1\left(\frac{b_i+b_j}{2}, b_j-b_i\right)$$

and variance

$$<\Delta\bar{\sigma}_1\left(\frac{b_i+b_j}{2}, b_j-b_i\right)^2> = \frac{1}{(b_i-b_j)^2}$$
$$\times\left[\sum_{j'=i}^{j-1} g_{ij'}^2\langle\Delta\tilde{\sigma}(h_{j'})^2\rangle + \sum_{j'=j}^{N}(g_{ij'}-g_{jj'})^2\langle\Delta\tilde{\sigma}(h_{j'})^2\rangle\right]. \quad (28)$$

From the calculation of $\bar{\sigma}_1(b, w)$ and $\langle\Delta\bar{\sigma}_1(b, w)^2\rangle$ we are now able to specify limits for $\bar{S}_1(b, w)$: $\bar{S}_1(b, w)$ lies, with a probability of approximately 0·86, within the range

$$\bar{\sigma}_1(b, w) - 1{\cdot}5\sqrt{\langle\Delta\bar{\sigma}_1(b, w)^2\rangle} \rightarrow \bar{\sigma}_1(b, w) + 1{\cdot}5\sqrt{\langle\Delta\bar{\sigma}_1(b, w)^2\rangle}\,.$$

It is generally found that the standard deviation

$$\frac{\sqrt{\langle\Delta\bar{\sigma}_1(b, w)^2\rangle}}{\langle\bar{\sigma}_1(b, w)\rangle}$$

decreases with increasing averaging range w; the limitation becomes narrower as the chosen value of w is increased.

To obtain information about the local values along the pinhole curve, a series of average values has to be computed. The following two different ways seem useful.

Firstly, a series of averaging distances $w(b_i)$ can be set and limitations for the course of $\bar{S}_1[b, w(b)]$ can be determined by computing the series of values

$$\bar{\sigma}_1\left(\frac{b_i+b_j}{2}, b_j-b_i\right)$$

and

$$<\Delta\bar{\sigma}_1\left(\frac{b_i+b_j}{2}, b_j-b_i\right)^2>\,, i=1, 2, \ldots, N\,,$$

where b_j is chosen as $b_j \simeq b_i + w(b_i)$. This seems especially suitable if it is assumed that $S_1(b)$ shows approximately linear character within distances of length $w(b)$ and thus remains almost unchanged by averaging over these distances.

Secondly, a condition can be set for the relative width of the limiting region, that means a certain precision of the results, and the minimum averaging distances $w_{\min}(b)$ needed to arrive at this precision, can be computed, together with the corresponding average values

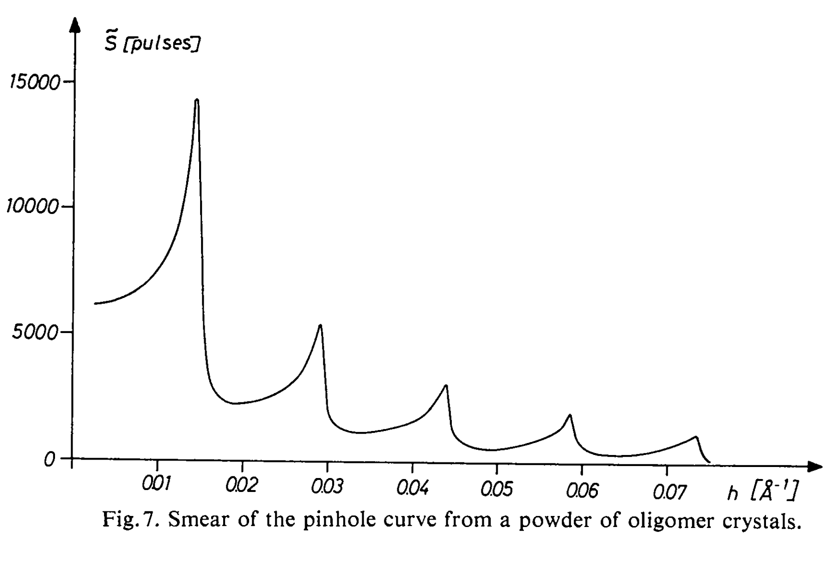

Fig. 7. Smear of the pinhole curve from a powder of oligomer crystals.

$\bar{\sigma}_1[b, w_{\min}(b)]$. The values $w_{\min}(b)$ then indicate how finely the pinhole curve has been resolved by the experiment; the values $\bar{\sigma}_1[b, w_{\min}(b)]$ fix, with the required precision, the course of $\bar{S}_1[b, w_{\min}(b)]$, and also that of

$$\bar{S}_0[b, w_{\min}(b)] \simeq \frac{1}{2b} \bar{S}_1[b, w_{\min}(b)]$$

[if $w_{\min}(b) \ll b$].

The evaluation procedures are applied directly to the measured data and there is no need for a preceding smoothing process. As a result of the errors (of random character) in the measured values, the calculated points will be found distributed over a certain range around the exact curve. A measure of the extent of this range is given by the calculated variances. It is this range of spread which clearly shows the limitations of the curve fitting, and thus the precision of the pinhole values.

Numerical examples

For demonstration two numerical examples have been calculated.

In the first example a curve of a form typical for semicrystalline polymeric substances is examined. Fig. 3 shows the smeared curve $S(h)$; we assumed registration to be in steps $\Delta h = 1{\cdot}5 \,.\, 10^{-4}$ Å^{-1} by counting the pulses during a fixed time, and a peak counting rate of roughly 10,000 pulses. Fig. 4 shows the result of applying equations (20) and (22) to calculate limits for the values of the integral intensity $T(b)$. In Fig. 5 the limits for $\overline{bS_0}(b, w = 1{\cdot}5 \,.\, 10^{-4}$ Å$^{-1})$ are given. The calculation was performed using equations (27) and (28). The curve shown in Fig. 6 is the original pinhole curve $S_0(b)$. The dashes represent average values

$$\int_{b_1}^{b_2} S_0(b')\mathrm{d}b'^2 \Big/ (b_2^2 - b_1^2)$$

of standard deviation less than 0·04, as calculated from the smeared curve. b_1 and b_2 are indicated by the beginning and the end of a dash respectively.

Since we started with the exact values $S(h_i)$ of the smeared curve, the use of the introduced formalism leads to the exact values $T(b_i)$ and $\overline{bS_0}(b_i, \Delta h) \simeq S_0(b_i) \,.\, b_i$. These lie in the middle of the plotted corresponding limiting curves. In a hypothetical measurement the measured values would be found spread around the exact curve $\tilde{S}(h)$. As a consequence, the points calculated by the application of the formulae to such a set of data would be found scattered within the regions limited by the drawn curves. Figs. 4, 5 & 6 clearly show the information content of the measurement. The intensity and the position of the main peak are well defined. Owing to the lower counting rates in the region around the second peak there is some uncertainty in the determination of its position and shape. Since the counting rates in the region $b = 0{\cdot}002$ Å$^{-1} \rightarrow b = 0{\cdot}005$ Å^{-1} are strongly influenced by the high peak intensity, the course of the pinhole curve in this range is only very roughly determined.

In a second example we deal with the smeared curve plotted in Fig. 7; we assumed registration in steps $\Delta h = 2{\cdot}25 \,.\, 10^{-4}$ Å^{-1} by counting the pulses during a fixed time; the intensities were chosen as indicated. Figs. 8 and 9 show the result of applying evaluation procedures to compute properties of the pinhole scattering curve in the region $b = 0{\cdot}005$ Å$^{-1} \rightarrow b = 0{\cdot}037$ Å^{-1}.

Calculation was done on the CD 3300 computer at the University of Mainz. The total computation time for calculating G^* and performing the evaluation procedures, resulting in the curves shown in Figs. 4, 5 and 6, lies in the range of 1 minute. A FORTRAN IV listing of the 'desmearing' program can be obtained from the author.

The author expresses his thanks to Professor E. W. Fischer for many valuable discussions and comments. He is much indebted to Dr P. Holdsworth for his advice in presenting these concepts. The work has been supported by the Deutsche Forschungsgemeinschaft.

APPENDIX

The condition-number of a matrix $\bar{\mathbf{g}}$ is defined as

$$\mathrm{cond}_\infty(\bar{\mathbf{g}}) = \frac{\mathrm{lub}_\infty \bar{\mathbf{g}}}{\mathrm{glb}_\infty \bar{\mathbf{g}}}$$

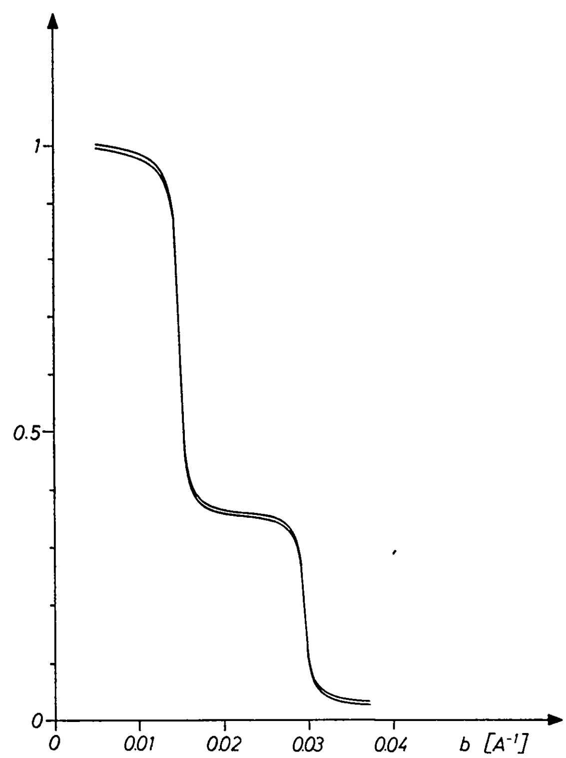

Fig. 8. Limiting curves for the integral intensity $T(b)$.

where

$$\text{lub}_\infty \bar{\mathbf{g}} = \sup_{\bar{\mathbf{S}}_0 \in \mathscr{R}^N} \frac{|\bar{\mathbf{g}} \cdot \bar{\mathbf{S}}_0|_\infty}{|\bar{\mathbf{S}}_0|_\infty} = \max_i \sum_j |\bar{g}(h_i, b_j)|$$

and

$$\text{glb}_\infty \bar{\mathbf{g}} = \inf_{\bar{\mathbf{S}}_0 \in \mathscr{R}^N} \frac{|\bar{\mathbf{g}} \cdot \bar{\mathbf{S}}_0|_\infty}{|\bar{\mathbf{S}}_0|_\infty} \, .$$

$\text{lub}_\infty(\bar{\mathbf{g}})$ can be easily calculated: it is, using equations (8), (3) and (5)

$$\sum_j |\bar{g}(h_i, b_j)| = \frac{1}{d} \int_{b=h}^{\infty} G(b^2 - h^2) \mathrm{d}b^2 = \frac{1}{d} 2C_1 L = \text{lub}_\infty \bar{\mathbf{g}}$$

where

$$L = \int_{-\infty}^{\infty} I(u) \mathrm{d}u$$

is a measure of the height of the primary beam.

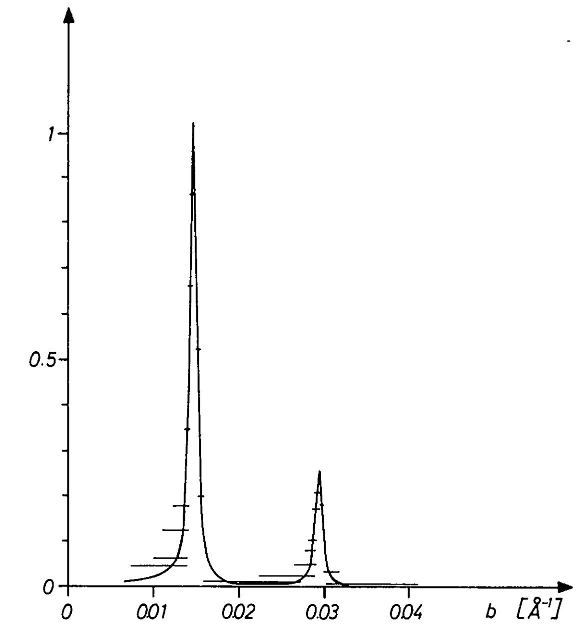

Fig. 9. A section of the original pinhole curve. The dashes represent average values as calculated from the smeared curve.

Since

$$\bar{g}(h_i, b_j) \geq 0$$

and, from equation (5),

$$\bar{g}(h_i, b_i) \geq \bar{g}(h_1, b_1) = 2V(0) \, , \quad \text{if} \quad V(d) \simeq V(0) \, ,$$

we get, for sufficiently small d, the inequality

$$|\bar{\mathbf{g}} \cdot \bar{\mathbf{S}}_0|_\infty \geq 2V(0) \cdot |\bar{\mathbf{S}}_0|_\infty \, .$$

For the special case $S_0(h_i) = \delta_{i1}$ we have

$$|\bar{\mathbf{g}} \cdot \bar{\mathbf{S}}_0|_\infty = 2V(0) \cdot |\bar{\mathbf{S}}_0|_\infty \, .$$

We therefore obtain

$$\text{glb}\bar{\mathbf{g}} = 2V(0) \, .$$

Hence, we get

$$\text{cond}_\infty(\bar{\mathbf{g}}) = \frac{C_1 L}{d \cdot V(0)} \, .$$

References

DuMond, J. W. (1947). *Phys. Rev.* **72**, 83.

Franklin, J. N. (1968). *Matrix Theory*, p. 174. Englewood Cliffs, New Jersey: Prentice-Hall.

Gerold, V. (1957). *Acta Cryst.* **10**, 287.

Guinier, A. (1963). *X-ray Diffraction*. London: Freeman & Co.

Guinier, A. & Fournet, G. (1947). *J. Phys. Radium*, **8**, 345.

Heine, S. & Roppert, J. (1962). *Acta Phys. Austriaca*, **15**, 148.

Hossfeld, F. (1968). *Acta Cryst.* **24**, 643.

Kent, P. & Brumberger, H. (1964). *Acta Phys. Austriaca*, **17**, 263.

Kratky, O., Porod, G. & Kahovec, L. (1951). *Z. Elektrochem.* **55**, 53.

Lake, J. A. (1967). *Acta Cryst.* **23**, 191.

Mazur, J. & Wims, A. M. (1966). *J. Res. Nat. Bur. Stand.* **70A**, 467.

Ruland, W. (1964). *Acta Cryst.* **17**, 138.

Schmidt, P. W. & Hight, R. (1960). *Acta Cryst.* **13**, 480.